Received: 22 January 2019 | Revised: 8 June 2019 | Accepted: 5 July 2019

DOI: 10.1002/rnc.4695

RESEARCH ARTICLE

WILEY

Adaptive backstepping-based control design for uncertain nonlinear active suspension system with input delay

Hui Pang | **Xu Zhang** | **Junjie Yang** | **Yuting Shang**

School of Mechanical and Precision Instrument Engineering, Xi'an University of Technology, Xi'an, China

Correspondence
Hui Pang, School of Mechanical and Precision Instrument Engineering, Xi'an University of Technology, Xi'an 710048, China.
Email: huipang@163.com

Funding information
National Natural Science Foundation of China, Grant/Award Number: 51675423 and 51305342; Primary Research & Development Plan of Shannxi Province, Grant/Award Number: 2017GY-029

Summary

This paper addresses the control problem of adaptive backstepping control for a class of nonlinear active suspension systems considering the model uncertainties and actuator input delays and presents a novel adaptive backstepping-based controller design method. Based on the established nonlinear active suspension model, a projector operator–based adaptive control law is first developed to estimate the uncertain sprung-mass online, and then the desirable controller design and stability analysis are conducted by combining backstepping technique and Lyapunov stability theory, which can not only deal with the actuator input delay but also achieve better dynamics performances and safety constraints requirements of the closed-loop control system. Furthermore, the relationship between the input delay and the state variables of this vehicle suspension system is derived to present a simple and effective method of calculating the critical input delay. Finally, a numerical simulation investigation is provided to illustrate the effectiveness of the proposed controller.

KEYWORDS

adaptive control, backstepping technique, input delay, nonlinear suspension system

1 | INTRODUCTION

It is well known that active suspension systems have been widely studied and implemented in vehicle application scenarios due to its advantages including the isolation, absorption, and dissipation of the vibration energies caused by road roughness.[1,2] Generally, the key issue of developing controller in active suspensions involves a trade-off between ride quality and road handling stability, which has been a subject of many research literatures.[3-5] Therefore, to deal with this issue, a number of control schemes such as adaptive fuzzy control,[6,7] robust H_∞ control,[8] slide mode control,[9,10] and adaptive backstepping control[11,12] have been proposed to improve the vehicle performance in the presence of system uncertainties and to minimize the negative effect of road disturbance on the control system.

In fact, a number of scholars have conducted the control design of active suspensions based on their linear models for the sake of simplicity and convenience of controller development.[13,14] However, it would be much more practical and

NOMENCLATURE: m_s, mass of vehicle body; z_s, sprung-mass displacement of vehicle body; $\dot{z}_s$, sprung-mass velocity of vehicle body; $\ddot{z}_s$, sprung-mass acceleration of vehicle body; $m_{s\min}$, the lower of vehicle body mass; $m_{s\max}$, the upper of vehicle body mass; F_c, damping force of suspension; F_s, stiffness force of suspension; k_s, nonlinear spring rigidity coefficient; k_{ns}, spatial stiffness coefficient of suspension; c_{s1}, extending damping coefficient of suspension; c_{s2}, compressing damping coefficient of suspension; k_t, stiffness coefficient of tire wheel; $\triangle y_{\max}$, the maximum of suspension dynamic displacement; m_u, unsprung mass of suspension; z_u, unsprung-mass displacement of vehicle body; $\dot{z}_u$, unsprung-mass velocity of the tire wheel; $\triangle y$, suspension dynamic displacement; z_r, road displacement disturbance of the tire wheel; $\dot{z}_r$, road velocity disturbance of the tire wheel; τ, time-varying input delay of actuator; $u(t\text{-}\tau)$, control force of the actuator with input delay; g, standard gravity acceleration; F_{static}, tire static load; F_{kt}, stiffness force of tire wheel; F_{ct}, damping force of tire wheel; c_t, distance from CG to the suspension; $u(t)_{\max}$, the maximum of actuator control force.

consistent with the actual situation if the spring and damper coefficients are taken as a nonlinear term, which is helpful to design an appropriate controller. Consequently, in the field of active suspension control, many researchers[15,16] have brought the nonlinear model of the spring and damper into the nonlinear active suspension model during the controller development process, in which the piecewise nonlinear spring force and the linear damper force are popularly used in the controller design for active suspension system.[17,18]

In nonlinear active suspension system, time delays are often encountered in the controlled channel, particularly in the digital controller as it carries out some calculations associated with the complex control law.[19] The existence of time delay may result in unexpected degradation in control performance and even instability.[20] Additionally, when modeling the real active suspension system, the model uncertainty generated from different vehicle body loads[21] is ubiquitous, and this may impose some difficulties in the implementation of the designed control scheme.

Among the abovementioned control methods during the latest several decades, the adaptive backstepping control, as an effective control scheme for a class of uncertain nonlinear system, has been widely and extensively investigated and reported in other works[22-25] because of such merits as anti-input saturation, interference suppression, accurate control, good robustness, etc. For instance, Khan et al[22] designed an efficient and novel adaptive neuro-fuzzy control or full car model with eight-degrees-of-freedom through the combination of the conventional adaptive backstepping technique and Mamdani fuzzy logic control, and the simulation results revealed that this control method can better improve the dynamical performances of vehicle suspension system compared to the linear-quadratic-regulated suspension systems. A nonlinear adaptive controller based on backstepping technique in the work of Nguyen et al[23] was presented to deal with the nonlinearity of the hydraulic actuator, whereas the suspension dynamic was linearly treated by H_∞ method. An adaptive position control method in the work of Ahn et al[24] was presented for a pump-controlled electrohydraulic actuator (EHA) based on adaptive backstepping control technology. In addition, the core feature of this study was the combination of a modified backstepping algorithm with a special adaptation law to compensate for all nonlinearities and uncertainties in EHA system. Zapateiro et al[25] have designed an optimal vibration controller for a class of vehicle suspension system with a magnetorheological actuator by combing the neural network and standard backstepping technique, which aimed to reduce the vibrations and enhance the suspension's performances. To sum up, the conventional adaptive backstepping control method has higher reliability in dealing with the ongoing variations of vehicle body masses, as well as the trajectory tracking error control of the grade-connection nonlinear system subjected to the external road disturbances.

On the other hand, there inevitably exists a time lag from the actuator to the plant, which will impose some negative effects on the controller performances.[26] Currently, the control design problems of active suspension system with the actuator time delay have attracted considerable attention due to the challenging issue of how to optimize the required suspension performances. Du and Zhang[27] have designed a constrained delay-dependent H_∞ state feedback controller to enhance the ride comfort, road holding ability, and stroke limitation performance to prescribed level regardless of a time delay in the control input, wherein the time delay was considered and assumed to be uncertain time invariant within a known constant bound. Li et al[28] have proposed a multiobjective H_∞ control for vehicle active suspension systems with random actuator delay, which can be represented by a signal probability distribution. Moreover, Du et al[29] have presented a parameter-dependent output feedback controller design for vehicle active suspensions to deal with changes in vehicle inertial properties and existence of actuator time delays, a good control performance was achieved within a certain range of time delay. In the work of Sun et al,[30] the problem of vehicle active suspension control with frequency band constraints and actuator input delay has been investigated and the controller design was transformed into a convex multiobjective optimization using LMI algorithm. To the best knowledge of the authors, only a few of studies on the adaptive backstepping control approaches were done for active suspension system with the actuator input delay. For example, the relevant study on the adaptive backstepping control design was described in literature,[31] wherein the full vehicle model with seven DOFs was taken as the control object with considering the time delay, and a Smith predictor was then employed to make a compensation for the time delay in this semi-active suspension system. However, the control effects of time delay on the suspension performances have not been addressed in the controller design, and the model uncertainties of suspension system are not considered.

Moreover, to the best of the authors' knowledge, the corresponding adaptive backstepping controller design is rarely reported in the published literatures, especially for nonlinear active suspension systems with the model uncertainties and the actuator input delays. Therefore, in order to cope with this problem, this paper addresses the control problem of adaptive backstepping control for a class of nonlinear active suspension systems considering the model uncertainties and actuator input delays. Based on the backstepping technique and Lyapunov stability theory, a novel adaptive backstepping-based controller is developed, and an evaluation approach for the critical input delay is presented.

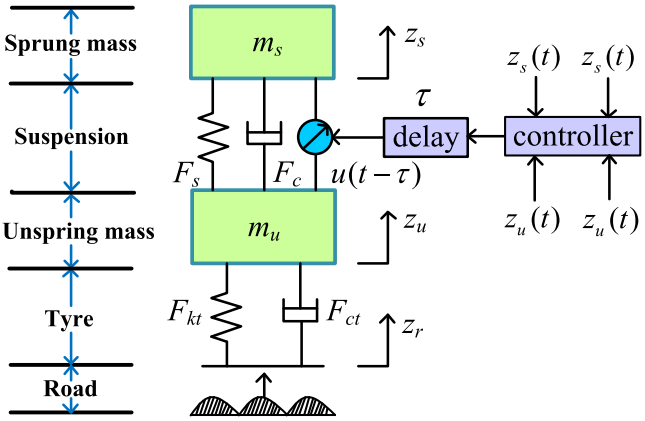

FIGURE 1 The nonlinear quarter-vehicle suspension model with input delay [Colour figure can be viewed at wileyonlinelibrary.com]

The proposed adaptive backstepping control scheme can guarantee that all the closed-loop signals are uniformly ultimately bounded. The main contributions of this paper are summarized as follows:

1. Different with the traditional adaptive backstepping controller in which the actuator input delay is rarely considered, the sprung-mass uncertainty and the actuator input delay, as well as the safety constraints of the nonlinear active suspension system, are taken into account simultaneously during the design process of our proposed novel adaptive backstepping-based controller.
2. The relationship between the input delay and state variables of the active suspension system is obtained through the theoretical derivations, and a solution method of the critical input delay is then presented, which is appropriate for the majority of the closed-loop control system.
3. The control stability is carried out by using Lyapunov theory to guarantee the asymptotic stability of the subsystem and the entire control system, thus further to obtain the upper bounds of each safety performance indicator, which reduce the conservativeness of the proposed controller.

The remainder of this paper is organized as follows. Section 2 presents system modeling of active suspension system and problem formulation. The proposed adaptive backstepping-based controller design with input delay is specifically discussed in Section 3. How to evaluate the critical input delay for the control plant is introduced in Section 4. In Section 5, the simulation investigation and discussion are presented to demonstrate the effectiveness and comparability of the designed controller. The conclusions are given in Section 6.

2 | SYSTEM MODELING AND PROBLEM STATEMENT

2.1 | System modeling of uncertain nonlinear active suspension

A quarter-vehicle model with the nonlinear spring and damping coefficients is considered and shown in Figure 1 with freedoms of motion in the heave directions, and this model has been extensively used in the previous literatures[28-30] due to its simplicity. Note that the input delay τ is a time-invariant unknown constant.

Based on Newton's second law, the dynamics equations of this control model are given by

$$\begin{cases} m_s\ddot{z}_s = -F_s\left(z_s, z_u, t\right) z_s - F_c\left(\dot{z}_s, \dot{z}_u, t\right) + u\left(t-\tau\right) \\ m_u\ddot{z}_u = F_s\left(z_s, z_u, t\right) + F_c\left(\dot{z}_s, \dot{z}_u, t\right) - u\left(t-\tau\right) \\ \qquad -F_{kt}\left(z_u, z_r, t\right) - F_{ct}\left(\dot{z}_u, \dot{z}_r, t\right). \end{cases} \tag{1}$$

Note that the mathematical expressions of nonlinear spring force $F_s(z_s, z_u, t)$ and the piecewise linear damper force $F_c\left(\dot{z}_s, \dot{z}_u, t\right)$ are, respectively, defined in (2) and (3),[32] and the tire elastic and damping forces of $F_{kt}(z_u, z_r, t)$ and $F_{ct}\left(\dot{z}_u, \dot{z}_r, t\right)$ are given in (4)[17] as follows:

$$F_s\left(z_s, z_u, t\right) = k_s\Delta y + k_{ns}\Delta y^3 \tag{2}$$

$$F_c\left(\dot{z}_s, \dot{z}_u, t\right) = \begin{cases} c_{s1}\Delta\dot{y}, \Delta\dot{y} > 0 \\ c_{s2}\Delta\dot{y}, \Delta\dot{y} \le 0 \end{cases} \tag{3}$$

$$\begin{cases} F_{kt}\left(z_u, z_r, t\right) = k_t\left(z_u - z_r\right) \\ F_{ct}\left(\dot{z}_u, \dot{z}_r, t\right) = c_t\left(\dot{z}_u - \dot{z}_r\right), \end{cases} \tag{4}$$

where $\Delta y = z_s - z_u$.

Define the state variables $x_1(t) = z_s$, $x_2(t) = \dot{z}_s$, $x_3(t) = z_u$, and $x_4(t) = \dot{z}_u$, then the state-space equations of vehicle body motion in (1) can be rewritten as

$$\begin{cases} \dot{x}_1(t) = x_2(t) \\ \dot{x}_2(t) = \frac{1}{m_s}\left(-F_s\left(z_s, z_u, t\right) - F_c\left(\dot{z}_s, \dot{z}_u, t\right) + u\left(t-\tau\right)\right) \\ \dot{x}_3(t) = x_4(t) \\ \dot{x}_4(t) = \frac{1}{m_u}(F_s\left(z_s, z_u, t\right) + F_c\left(\dot{z}_s, \dot{z}_u, t\right) - F_{kt}\left(z_u, z_r, t\right) \\ \qquad -F_{ct}\left(\dot{z}_u, \dot{z}_r, t\right) - u\left(t-\tau\right)). \end{cases} \tag{5}$$

2.2 | Problem statement of the control system

For the control plant, m_s is determined as the uncertain parameter in the active suspension system of (5) due to the variations of passenger numbers and vehicle body loads, and suppose that the lower and upper bounds of m_s, denoted as $m_{s\min}$ and $m_{s\max}$, satisfy

$$m_s \in \left\{m_s : m_{s\min} \le m_s \le m_{s\max}\right\}.$$

Herein, the key objective of this work is to design an effective finite-time control law, which can not only deal with the tolerable input delay but also stabilize the vertical acceleration of vehicle body. By following the related studies in the works of Sun et al,[33-35] in order to ensure that the controlled active suspension system has better dynamic performances such as the ride comfort and handling capacity, the performance requirements to be considered in the controller design include the following two aspects:

(i) Ride comfort: The designed controller can achieve the asymptotic convergence of the vertical acceleration within a finite time in the presence of the uncertain parameters m_s and the input delay τ in (5).

(ii) Safety performance constraints

① Suspension space limits: Considering the limit of suspension mechanical structure, the suspension dynamic displacement should be restrained within its allowable maximum value, which is expressed by

$$|\Delta y| \le \Delta y_{\max}. \tag{6}$$

② Road holding ability: To ensure vehicle riding safety, the dynamic loads of the tire should not exceed static loads, which is given by

$$F_{\text{radio}} = \left|k_t\left(z_u - z_r\right) + c_t\left(\dot{z}_u - \dot{z}_r\right)\right| / F_{\text{static}} < 1, \tag{7}$$

where $F_{\text{static}} = (m_s + m_u)g$.

③ Actuator saturation: The amplitude of control force generated by the actuator should be restrained in a reasonable range. If the limitation exceeded, the performance of the closed-loop system (5) will be degraded or even unstable, the related-input delay control force is given by

$$|u\left(t-\tau\right)| \le u(t)_{\max}. \tag{8}$$

Assumption 1. The external unknown disturbance $Z_r(t)$ satisfies $\|Z_r(t)\| \le \bar{d}$, where $\bar{d} > 0$ is an unknown constant.

Remark 1. Assumption 1 is used to clarify the boundedness of the real control input and the external disturbance, and it is noted that this assumption is reasonable in most of the nonlinear output feedback system under normal working conditions.

3 | ADAPTIVE BACKSTEPPING-BASED CONTROL DESIGN

In this section, the control problem formulated in Section 2 will be solved by designing a nonlinear adaptive backstepping controller that is able to guarantee the following requirements:

1. The proposed controller can succeed in stabilizing the vertical motion of vehicle body and isolating the force transmitted to the passengers in the presence of the uncertain parameters and the external disturbances.

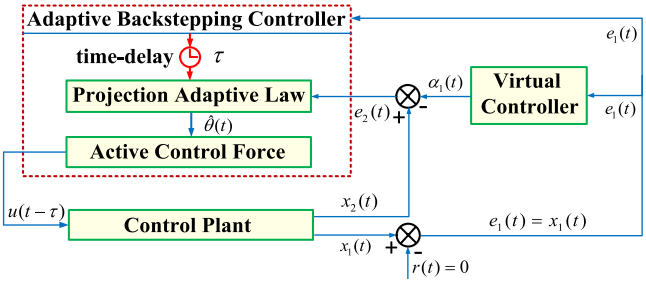

FIGURE 2 The control diagram of the proposed adaptive backstepping controller [Colour figure can be viewed at wileyonlinelibrary.com]

2. The required suspension safety performance constraints such as suspension space limit in (8), ride safety condition in (9), and actuator saturation in (10) can be definitely satisfied.

3.1 | Adaptive control scheme

In the first place, the proposed adaptive backstepping control diagram is presented in Figure 2, wherein the control plant, the virtual controller, the projection adaptive law, and the active control force are included. Note that the control variables are the vertical displacement $x_1(t)$ and the vertical velocity of vehicle body $x_2(t)$, respectively. Next, it is necessary to establish the error of the vehicle sprung-mass displacement denoted as $e_1(t)$, whereby the predetermined virtual control $\alpha_1(t)$ is employed to ensure the suspension performances; and the error of the sprung-mass velocity denoted as $e_2(t)$, which is taken as the input of projection adaptive law $\hat{\theta}(t)$ that is used to eliminate the effect caused by the sprung-mass uncertainty. Finally, the related-input delay control force $u(t-\tau)$ is designed to make $e_1(t)$ and $e_2(t)$ be convergent and stable with $t \to \infty$, wherein $r(t) = 0$ is zero reference value.

To facilitate the controller design and stability analysis, Lemma 1 is presented in the following.

Lemma 1 (See the work of Sun[36]). *If a general error variable e(t) (ie, $e_1(t)$ or $e_2(t)$ in this work) is uniformly continuous and $\lim_{t\to\infty} \int_0^t e(s)\,ds$ exists with a finite bound, then one has $\lim_{t\to\infty} e(t) \to 0$, which is an extended derivation of Barbalat lemma, extensively appearing in the literature of control theory.*

3.2 | Controller design and stability analysis

Overall, we need to design an appropriate adaptive backstepping controller consisting of the control input $u(t-\tau)$ and the adaptive law $\dot{\hat{\theta}}(t)$ with aiming to inhibit the vibrations caused by the input delay and the uncertain parameter of body mass. To that end, the controller design is achieved by the sequential four steps as follows.

First, by introducing the zero reference value of $x_1(t)$, one can easily obtain $e_1(t) = x_1(t)$ and then design a virtual control function $\alpha_1(t)$ satisfying $x_2(t) = \alpha_1(t)$ so as to make $e_1(t)$ tend to stability within a finite time, and meanwhile, define the error of $e_2(t)$ between the actual state $x_2(t)$ and the virtual input $\alpha_1(t)$, we have

$$e_2(t) = x_2(t) - \alpha_1(t) = \dot{x}_1(t) - \alpha_1(t). \tag{9}$$

Afterwards, define a semidefinite Lyapunov candidate function $V_1(e_1(t))$ as

$$V_1 = \frac{1}{2} e_1^2(t). \tag{10}$$

Following the design of the virtual control function $\alpha_1(t)$, we have

$$\alpha_1(t) = -k_1 \tanh(e_1(t)), \tag{11}$$

where k_1 is a positive constant.

Differentiating (10) gives

$$\dot{V}_1(e_1(t)) = e_1(t) e_2(t) - k_1 e_1(t) \tanh(e_1(t)). \tag{12}$$

From (12), if $e_2(t) = 0$, thus we can derive that $\dot{V}_1(e_1(t)) = -k_1 e_1(t) \tanh(e_1(t)) \leq -k_1 e_1^2(t) \leq 0$ holds, and it is consequently easy to guarantee $e_1(t)$ reach a stability state asymptotically.

Second, design $u(t-\tau)$ in system (5) to make $\dot{x}_1(t)$ well track the evaluation of $\alpha_1(t)$ in the presence of the uncertain parameter θ_1 of m_s.

By taking the time derivative $e_2(t)$ in (9), one obtains

$$\dot{e}_2(t) = \theta\delta_1(x,t) - \dot{\alpha}_1(t), \tag{13}$$

where $\delta_1(x,t) = -F_c(z_s, z_u, t) - F_s(\dot{z}_s, \dot{z}_u, t) + u(t-\tau)$, and $\theta = 1/m_s \in [\theta_{\min}, \theta_{\max}]$, $\theta_{\min} = 1/m_{s\max}$, $\theta_{\max} = 1/m_{s\min}$.

Herein, the Lyapunov function is selected as

$$V_2(e_1, e_2, \tilde{\theta}, t) = V_1(e_1(t)) + \frac{1}{2}e_2^2(t) + \frac{1}{2r_\theta}\tilde{\theta}^2(t), \tag{14}$$

where $\tilde{\theta}(t) = \widehat{\theta}(t) - \theta$ is the difference between the estimated parameter $\widehat{\theta}(t)$ and the real value θ.

Differentiating Equation (14) yields to

$$\begin{aligned}\dot{V}_2(e_1, e_2, \tilde{\theta}, t) &= \dot{V}_1(e_1(t)) + e_2(t)\dot{e}_2(t) + r_\theta^{-1}\tilde{\theta}(t)\dot{\hat{\theta}}(t)\\ &= e_1(t)e_2(t) - k_1e_1(t)\tanh(e_1(t)) + e_2(t)\dot{e}_2(t) + r_\theta^{-1}\tilde{\theta}(t)\dot{\hat{\theta}}(t)\\ &= e_2(t)(e_1(t) - \theta\Delta_1(x,t) - \dot{\alpha}_1(t)) - k_1e_1(t)\tanh(e_1(t)) + r_\theta^{-1}\tilde{\theta}(t)\dot{\hat{\theta}}(t).\end{aligned} \tag{15}$$

If we choose the control law $u(t-\tau)$ as

$$u(t-\tau) = F_c(z_s, z_u, t) + F_s(\dot{z}_s, \dot{z}_u, t) + \frac{1}{\hat{\theta}(t)}(\dot{\alpha}_1(t) - k_2\tanh(e_2(t)) - e_1(t)), \tag{16}$$

where k_2 is a positive constant, then we have

$$\dot{V}_2(e_1, e_2, \tilde{\theta}, t) = -k_1e_1(t)\tanh(e_1(t)) - k_2e_2(t)\tanh(e_2(t)) + \tilde{\theta}(t)\left(r_\theta^{-1}\dot{\hat{\theta}}(t) - e_2(t)\Delta_1(x,t)\right). \tag{17}$$

Based on the projection operator,[37,38] the adaptive control law $\dot{\hat{\theta}}(t)$ is defined as

$$\dot{\hat{\theta}}(t) = \mathrm{proj}_{\hat{\theta}}(r_\theta e_2(t)\Delta_1(x,t)) = \begin{cases} 0, & \text{if } \hat{\theta}(t) = \theta_{\max} \text{ and } r_\theta e_2(t)\Delta_1(x,t) > 0\\ 0, & \text{if } \hat{\theta}(t) = \theta_{\min} \text{ and } r_\theta e_2(t)\Delta_1(x,t) < 0\\ r_\theta e_2(t)\Delta_1(x,t), & \text{othercase,}\end{cases} \tag{18}$$

where $r_\theta > 0$ is the tuning parameter for the adaptive control law $\mathrm{proj}_{\hat{\theta}}(r_\theta e_2(t)\Delta_1(x,t))$.

Remark 2. The projection operator–based adaptive control law $\mathrm{proj}_{\hat{\theta}}(r_\theta e_2(t)\Delta_1(x,t))$ has the following three main features:

① The parameter estimation $\widehat{\theta}(t)$ can be always ensured within a known range, ie, $\theta_{\min} < \hat{\theta}(t) < \theta_{\max}$.

② The hold of $\tilde{\theta}(t)(r_\theta^{-1}\mathrm{proj}_{\hat{\theta}}(r_\theta e_2(t)\Delta_1(x,t)) - e_2(t)\delta_1(x,t)) \le 0$ can be always guaranteed.

③ A constrained function of $\tanh(e_i)$ is used to replace the linear feedback term e_i with the purpose of avoiding the safety constraints going beyond its limits that are caused by the overlarge tracking error e_i.

In (18), the online estimation of m_s can be realized by selecting an appropriate value of r_θ and $\theta(0)$ for the closed-loop system, and then the influence of uncertain sprung mass on the system stability can be further eliminated, which guarantees the being of $\theta_{\min} < \hat{\theta}(t) < \theta_{\max}$.

Furthermore, we can obtain

$$\dot{V}_2(e_1, e_2, \tilde{\theta}, t) = -k_1e_1(t)\tanh(e_1(t)) - k_2e_2(t)\tanh(e_2(t)) \le 0. \tag{19}$$

Next, we will perform the following proof so as to ensure that the tracking errors of $e_1(t)$ and $e_2(t)$ can achieve the stability state within a finite time by using the designed control input $u(t-\tau)$ and the adaptive control law $\dot{\hat{\theta}}(t)$.

For the inequality of $\dot{V}_2(e_1, e_2, \tilde{\theta}, t) \leq 0$, integrating both of the sides in (19) from the range of 0 to t simultaneously, we can get

$$\begin{aligned} V_2(e_1, e_2, \tilde{\theta}, t) &= \int_0^t \dot{V}_2(e_1, e_2, \tilde{\theta}, t) d\tau + V_2(e_{,1}(0)\, e_2(0)\, \tilde{\theta}(0)) \\ &\leq V_2(e_{,1}(0)\, e_2(0)\, \tilde{\theta}(0)). \end{aligned} \tag{20}$$

It can be observed that $e_1(0)$ and $e_2(0)$ are bounded, which is expressed in the following forms:

$$\begin{cases} |e_1(t)| \leq \sqrt{2V_2(e_{,1}(0)\, e_2(0)\, \tilde{\theta}(0))}, \\ |e_2(t)| \leq \sqrt{2V_2(e_{,1}(0)\, e_2(0)\, \tilde{\theta}(0))}. \end{cases} \tag{21}$$

Meanwhile, $\tilde{\theta}_1(0)$ is also bounded, from (21), we can further get

$$\begin{cases} |x_1(t)| \leq \sqrt{2V_2(e_{,1}(0)\, e_2(0)\, \tilde{\theta}(0))} \\ |x_2(t)| \leq (k_1+1)\sqrt{2V_2(e_{,1}(0)\, e_2(0)\, \tilde{\theta}(0))}. \end{cases} \tag{22}$$

Thus, we have

$$-F_s(z_s, z_u, t) - F_c(\dot{z}_s, \dot{z}_u, t) + u(t-\tau) \in L_\infty. \tag{23}$$

Henceforth, we get $\dot{e}_2 \in L_\infty$ and

$$\begin{aligned} \ddot{V}_2(e_1, e_2, \tilde{\theta}, t) \leq & -k_1 e_1(t)(1-\tanh^2(e_1(t)))\dot{e}_1(t) - k_1 \dot{e}_1(t)\tanh(e_1(t)) \\ & -k_2 e_2(t)(1-\tanh^2(e_2(t)))\dot{e}_2(t) - k_2 \dot{e}_2(t)\tanh(e_2(t)). \end{aligned} \tag{24}$$

Remark 3. From (22), we obtain the conclusions that $\ddot{V}_2 \in L_\infty$and $\dot{V}_2$ are uniformly continuous. Moreover, it can be derived from Lemma 1 that it is true for $\lim_{t\to\infty} \dot{V}_2 \to 0$ with $t \to \infty$, the further expressions are $\lim_{t\to\infty} e_1(t) \to 0$ and $\lim_{t\to\infty} e_2(t) \to 0$. In other words, we can arrive at the conclusion that the tracking errors of $e_1(t)$ and $e_2(t)$ will definitely tend to be asymptotic stability.

Third, it is needed to conduct the stability analysis of zero dynamics for the controlled suspension system.

Since Equation (5) is composed of a four-order system, the error system in the proposed controller is a two-order system. Therefore, the zero dynamics system consists of two state variables of $x_3(t)$ and $x_4(t)$. To find out the zero dynamics, the tracking error of $e_1(t)$ is set to zero, ie, $e_1(t) = 0$, thus we have $e_2(t) = 0$ and the following equation:

$$u(t-\tau) = F_s(z_s, z_u, t) + F_c(\dot{z}_s, \dot{z}_u, t). \tag{25}$$

Substituting Equation (25) into Equation (5) gives

$$\begin{cases} \dot{x}_3 = x_4, \\ \dot{x}_4 = \frac{1}{m_u}(F_s(z_s, z_u, t) + F_c(\dot{z}_s, \dot{z}_u, t) - u(t-\tau(t)) \\ \qquad -k_t(z_u - z_r) - c_t(\dot{z}_u - \dot{z}_r)). \end{cases} \tag{26}$$

The zero dynamics equation can be obtained as follows:

$$\dot{X}(t) = \boldsymbol{A}X(t) + \boldsymbol{B}Z_r(t), \tag{27}$$

where $\boldsymbol{X}(t) = [x_3(t), x_4(t)]^{\mathrm{T}}$ and

$$\boldsymbol{A} = \begin{bmatrix} 0 & 1 \\ -\frac{k_t}{m_u} & -\frac{c_t}{m_u} \end{bmatrix}, \boldsymbol{B} = \begin{bmatrix} 0 & 0 \\ \frac{k_t}{m_u} & \frac{c_t}{m_u} \end{bmatrix}, Z_r(t) = [z_r(t) \quad \dot{z}_r(t)]^{\mathrm{T}}.$$

By defining the positive definite function as $V_3 = \boldsymbol{X}^{\mathrm{T}}(t)\boldsymbol{P}\boldsymbol{X}(t)$, wherein $\boldsymbol{P}$ is a positive definite matrix, then we have

$$\begin{aligned} \dot{V}_3(x(t)) &= \dot{\boldsymbol{X}}^{\mathrm{T}}(t)\boldsymbol{P}\boldsymbol{X}(t) + \boldsymbol{X}^{\mathrm{T}}(t)\boldsymbol{P}\dot{\boldsymbol{X}}(t) \\ &= \boldsymbol{X}^{\mathrm{T}}(t)\left(\boldsymbol{A}^{\mathrm{T}}\boldsymbol{P} + \boldsymbol{P}\boldsymbol{A}\right)\boldsymbol{X}(t) + 2\boldsymbol{X}^{\mathrm{T}}(t)\boldsymbol{P}\boldsymbol{B}Z_r(t). \end{aligned} \tag{28}$$

Since the eigenvalues of the real parts for matrix $\boldsymbol{A}$ are all negative values, thus one can get $\boldsymbol{A}^{\mathrm{T}}\boldsymbol{P} + \boldsymbol{P}\boldsymbol{A} = -\boldsymbol{Q}$, where $\boldsymbol{Q}$ is a positive definite matrix.[17] Moreover, the following inequality of (29) holds as

$$2\boldsymbol{X}^{\mathrm{T}}(t)\boldsymbol{P}\boldsymbol{B}\boldsymbol{Z}_r(t) \le \frac{1}{v_1}\boldsymbol{X}^{\mathrm{T}}(t)\boldsymbol{P}\boldsymbol{B}\boldsymbol{B}^{\mathrm{T}}\boldsymbol{P}\boldsymbol{X}(t) + v_1\boldsymbol{Z}_r^{\mathrm{T}}(t)\boldsymbol{Z}_r(t). \tag{29}$$

In (29), v_1 is an adjustable parameter, and then we can deduce from (28) and (29) that the following inequality holds:

$$\begin{aligned} \dot{V}_3(x(t)) &\le -\boldsymbol{X}^{\mathrm{T}}(t)\boldsymbol{Q}\boldsymbol{X}(t) + \frac{1}{v_1}\boldsymbol{X}^{\mathrm{T}}(t)\boldsymbol{P}\boldsymbol{B}\boldsymbol{B}^{\mathrm{T}}\boldsymbol{P}\boldsymbol{X}(t) + v_1\boldsymbol{Z}_r^{\mathrm{T}}(t)\boldsymbol{Z}_{\boldsymbol{r}}(t) \\ &\le \left[-\lambda_{\min}\left(\boldsymbol{P}^{-\frac{1}{2}}\boldsymbol{Q}\boldsymbol{P}^{-\frac{1}{2}}\right) + \frac{\lambda_{\max}}{v_1}\left(\boldsymbol{P}^{\frac{1}{2}}\boldsymbol{B}\boldsymbol{B}^{\mathrm{T}}\boldsymbol{P}^{\frac{1}{2}}\right)\right]V_3(x(t)) + v_1\boldsymbol{Z}_r^{\mathrm{T}}(t)\boldsymbol{Z}_r(t). \end{aligned} \tag{30}$$

Selecting matrix $\boldsymbol{P}$ and $\boldsymbol{Q}$ with the appropriate dimensions and a tunable parameter v_1 can guarantee

$$\lambda_{\min}\left(\boldsymbol{P}^{-\frac{1}{2}}\boldsymbol{Q}\boldsymbol{P}^{-\frac{1}{2}}\right) - \frac{\lambda_{\max}}{v_1}\left(\boldsymbol{P}^{\frac{1}{2}}\boldsymbol{B}\boldsymbol{B}^{\mathrm{T}}\boldsymbol{P}^{\frac{1}{2}}\right) \ge \beta_1, \tag{31}$$

where β_1 is a positive constant.

Define $\boldsymbol{Z}_r^{\mathrm{T}}(t)\boldsymbol{Z}_r(t) \le \boldsymbol{Z}_{r\max}$ so as to get

$$v_1\boldsymbol{Z}_r^{\mathrm{T}}(t)\boldsymbol{Z}_r(t) \le v_1\boldsymbol{Z}_{r\max} = \beta_2. \tag{32}$$

Thus far, we can obviously get $\dot{V}_3(x(t)) \le -\beta_1 V_3(x(t)) + \beta_2$ and the following inequality:

$$V_3(x(t)) \le \left(V_3(x(0)) - \frac{\beta_2}{\beta_1}\right)e^{-\beta_1 t} + \frac{\beta_2}{\beta_1}. \tag{33}$$

It is clear from (33) that there exists a known boundary in $V_3(x(t))$, and meanwhile, we have

$$|x_k(t)| \le \sqrt{\frac{q}{\lambda_{\min}(\boldsymbol{P})}}, (k = 3, 4), \tag{34}$$

where

$$q = \begin{cases} V_3(x(0)), & \text{if } V_3(x(0)) \ge \frac{\beta_2}{\beta_1} \\ \frac{2\beta_2}{\beta_1} - V_3(x(0)), & \text{if } V_3(x(0)) < \frac{\beta_2}{\beta_1}. \end{cases}$$

It can be concluded from the above three steps that all of the state variables have a certain boundary, and all the upper boundaries can be estimated.

Fourth, determine the adjustable parameter selection law to ensure the satisfaction of the safety performance constraints for the controlled suspension system, which is described as the following aspects:

1. The upper bound of suspension dynamic displacement can be estimated by

$$|z_s - z_u| \leq |x_1(t)| + |x_3(t)| \leq \sqrt{2V_2\left(e_{,1}(0)\, e_2(0)\, \tilde{\theta}(0)\right)} + \sqrt{\frac{q}{\lambda_{\min}(\boldsymbol{P})}} = \eta_1. \tag{35}$$

2. The upper bound of tire dynamic load can be estimated by

$$\begin{aligned} |k_t(z_u - z_r) + c_t(\dot{z}_u - \dot{z}_r)| &\leq k_t|x_3(t)| + k_t|z_r| + c_t|x_4(t)| + c_t|\dot{z}_r| \\ &\leq \frac{(k_t + c_t)\sqrt{q}}{\lambda_{\min}(\boldsymbol{P})} + k_t\|z_r\|_\infty + c_t\|\dot{z}_r\|_\infty = \eta_2. \end{aligned} \tag{36}$$

3. The upper bound of the control input can be estimated by

$$|u(t-\tau)| \leq \frac{1}{\theta_{\min}}\left(k_1|\dot{e}_1(t)| + k_2|e_2(t)| + |e_2(t)|\right) + \left|F_{,s}(z_s z_u t)\right| + |F_c(\dot{z}_s, \dot{z}_u, t)| = \eta_3. \tag{37}$$

It is worth pointing out that the safety performance constraints mentioned in the control objectives can be guaranteed through setting an appropriate value of v_1 and the tuning gains of k_1, k_2 simultaneously make the inequalities of (38) to (40) below hold

$$|z_s - z_u| \leq \eta_1 \leq \Delta y_{\max} \tag{38}$$

$$F_{\text{radio}} = \frac{|k_t(z_u - z_r) + c_t(\dot{z}_u - \dot{z}_r)|}{\eta_2} \leq 1 \tag{39}$$

$$|u(t-\tau)| \leq \eta_3 \leq u(t)_{\max}, \tag{40}$$

wherein $\Delta y_{\max} = 0.15$ m and $u(t)_{\max} = 1000$ N. Thus far, the adaptive backstepping controller design can be concluded as Theorem 1 as follows.

Theorem 1. *Consider the nonlinear active suspension system in (5), the implementation of the designed control laws in (18) can ensure the following safety performance constraints:*

1. The closed-loop system (5) is asymptotically stable, ie, all the output signals tend to stability gradually with $t \to \infty$.

2. Only if the initial values of the system (5) satisfy the constraint conditions in (38)-(40), the suspension performance constraints as given in (6)-(8) can be guaranteed.

Remark 4. In this section, a novel adaptive backstepping controller that can inhibit the input delay is developed based on Lyapunov stability theory, which is presented in Step 1 to Step 4. Moreover, this designed controller can guarantee the global asymptotic stability and the stability of zero dynamics of the closed-loop system, and further guarantee that all the control signals are bounded in a certain range and the upper bounds of each variable are estimable. In addition to this, the safety performances in the control objects can be ensured by giving an appropriate control gain.

4 | PERFORMANCE EVALUATION OF THE PROPOSED CONTROLLER

It is generally accepted the fact that the excessive input delay may usually lead to the instability of the designed controller. To further investigate the influence of input delay τ on the suspension performance, the critical input delay of the actuator, denoted as $\tau_{\max}$, should be evaluated based on the linearization principle of the nonlinear system[39] and the vibration control theory.[40]

4.1 | The calculation method of the critical input delay

First, as shown in Equation (2) and Equation (3), the nonlinear spring and damping forces F_s and F_c are related to the vertical displacement and velocity of vehicle body, respectively. These two nonlinear forces can be linearized without

considering the actuator input delay and the root-means-square (RMS) for F_s and F_c that is related to the vertical displacement and velocity of active suspension system can be further mathematically expressed by

$$\begin{cases} F_s(z_s, z_u, t)_{\mathrm{RMS}} = \sqrt{\frac{1}{n}\sum_{i=1}^{n}\left(F_s\left(z_s, z_u, t\right)\right)^2} \\ F_c(\dot{z}_s, \dot{z}_u, t)_{\mathrm{RMS}} = \sqrt{\frac{1}{n}\sum_{i=1}^{n}\left(F_s\left(\dot{z}_s, \dot{z}_u, t\right)\right)^2} \\ \Delta y(t)_{\mathrm{RMS}} = \sqrt{\frac{1}{n}\sum_{i=1}^{n}\left(\Delta y\left(t\right)\right)^2} \\ \Delta \dot{y}(t)_{\mathrm{RMS}} = \sqrt{\frac{1}{n}\sum_{i=1}^{n}\left(\Delta \dot{y}\left(t\right)\right)^2}. \end{cases} \tag{41}$$

Second, in terms of linearization theory,[39] the force feedback coefficients are introduced to derive the new and simple expression of F_s and F_c as follows:

$$F_s\left(z_s, z_u, t\right) = l_s \Delta y \tag{42}$$

$$F_c\left(\dot{z}_s, \dot{z}_u, t\right) = l_c \Delta \dot{y}, \tag{43}$$

where l_s and l_c are the feedback coefficients to be determined, respectively.

However, it is noticed that, in a certain control scheme, the corresponding control force can be obtained by determining the appropriate control variable's values. For this controller design, if we carry out the selection of the suitable control variables satisfying $e_1(t) \to x_1(t)$, $e_2\left(t\right) \to \dot{x}_1\left(t\right)$, the desirable active control force $u(t-\tau)$ can be obtained during the adaptive control design process in Section 3.2. Specifically, when the closed-loop system is input delay-free, that is $\tau = 0$, the expression of the control input $u(t)$ is given by

$$u\left(t\right) = l_1 x_1\left(t\right) - l_2 \dot{x}_1\left(t\right), \tag{44}$$

where l_1 and l_2 are the feedback coefficients to be determined.

Based on the abovementioned analysis and discussion, we can get Remark 4 as follows.

Remark 5. It is well known that the suitable feedback coefficients are significantly to derive the ideal control input $u(t)$,[41] after some iterative calculations and comparative analysis for this case, we found out that the bump signal has a greater effect on the dynamics performance of active suspension system in (5) compared to the random signal. Therefore, it is necessary to calculate the desired l_1 and l_2 to further evaluate the critical input delay $\tau_{\max}$.

By taking some calculations, we get $l_s = 15166$ N/m, $l_c = 1313$ Ns/m, $l_1 = 2720$ N/m, $l_2 = -1268$ Ns/m, which will be used in the subsequent solution of $\tau_{\max}$. Substituting Equations (42)-(44) into Equation (1), we can obtain

$$\begin{cases} m_s \ddot{z}_s\left(t\right) = -l_s \Delta y - l_c \Delta \dot{y} + l_1 z_s\left(t-\tau_{\max}\right) - l_2 \dot{z}_s\left(t-\tau_{\max}\right) \\ m_u \ddot{z}_u\left(t\right) = l_s \Delta y + l_c \Delta \dot{y} - l_1 z_s\left(t-\tau_{\max}\right) + l_2 \dot{z}_s\left(t-\tau_{\max}\right) \\ \qquad\qquad - k_t\left(z_u\left(t\right) - z_r\left(t\right)\right) - c_t\left(\dot{z}_u\left(t\right) - \dot{z}_r\left(t\right)\right). \end{cases} \tag{45}$$

To derive the calculation expression of $\tau_{\max}$, we rewrite Equation (45) by removing the external road disturbance z_r and $\dot{z}_r$ as follows:

$$\begin{cases} m_s \ddot{z}_s\left(t\right) = -l_s \Delta y - l_c \Delta \dot{y} + l_1 z_s\left(t-\tau_{\max}\right) - l_2 \dot{z}_s\left(t-\tau_{\max}\right) \\ m_u \ddot{z}_u\left(t\right) = l_s \Delta y + l_c \Delta \dot{y} - l_1 z_s\left(t-\tau_{\max}\right) + l_2 \dot{z}_s\left(t-\tau_{\max}\right) \\ \qquad\qquad - k_t z_u\left(t\right) - c_t \dot{z}_u\left(t\right). \end{cases} \tag{46}$$

Applying the basic vibration analysis theory, the solutions of Equation (46) can be given as

$$\begin{cases} z_s\left(t\right) = z_{10} e^{\omega t} = z_{10} e^{\left(\sigma + j\omega_c\right)t} \\ z_u\left(t\right) = z_{20} e^{\omega t} = z_{20} e^{\left(\sigma + j\omega_c\right)t}, \end{cases} \tag{47}$$

where $w = \sigma + j\omega_c$ is the complex mode frequency, z_{10} and z_{20} are the initial values of the eigenvector in (46), respectively, σ is the attenuation coefficient, and ω_c is the natural frequency for the closed-loop system in (46).

Substituting Equation (47) into Equation (46) generates the coefficient matrix determinant as follows:

$$\begin{bmatrix} z_{11} & z_{12} \\ z_{21} & z_{22} \end{bmatrix} \begin{bmatrix} z_{10} \\ z_{20} \end{bmatrix} = \begin{bmatrix} 0 \\ 0 \end{bmatrix}, \tag{48}$$

where

$$z_{11} = (\sigma + j\omega_c)^2 m_s + l_c(\sigma + j\omega_c) + l_s - \left[l_1 - l_2(\sigma + j\omega_c)\right] e^{-(\sigma + j\omega_c)\tau_{\max}},$$

$$z_{12} = -l_s - l_c(\sigma + j\omega_c),$$

$$z_{21} = -l_s - l_c(\sigma + j\omega_c) + \left[l_1 - l_2(\sigma + j\omega_c)\right] e^{-(\sigma + j\omega_c)\tau_{\max}},$$

$$z_{22} = (\sigma + j\omega_c)^2 m_u + (l_c + c_t)(\sigma + j\omega_c) + l_s + k_t.$$

If Equation (48) has a nonzero solution, then the following condition should be satisfied

$$\begin{vmatrix} z_{11} & z_{12} \\ z_{21} & z_{22} \end{vmatrix} = 0. \tag{49}$$

By using the Euler formula to simplify (49), the corresponding solutions can be expressed in the form of $a + bj = 0$. The real part a and the imaginary part b are separated and assumed to be zero, thus the value of σ and ω_c can be solved in terms of this equation. It is noted that the value of σ includes three situations as $\sigma < 0$, $\sigma = 0$, and $\sigma > 0$.

When $\sigma < 0$, the closed-loop system is stable, and for $\sigma = 0$, the system is critically stable; and for $\sigma > 0$, the system is unstable. For this reason, this article mainly focuses on the solving of ω_c and $\tau_{\max}$, then substituting $\sigma = 0$ into Equation (49) forms

$$\begin{vmatrix} -\omega_c^2 m_s + l_c j\omega_c + l_s - (l_1 - l_2 j\omega_c) e^{-j\omega_c \tau_{\max}} & -l_s - l_c j\omega_c \\ -l_s - l_c j\omega_c + (l_1 - l_2 j\omega_c) e^{-j\omega_c \tau_{\max}} & -\omega_c^2 m_u + (l_c + c_t) j\omega_c + l_s + k_t \end{vmatrix} = 0. \tag{50}$$

By taking further transformations, we have

$$\begin{cases} \omega_c^4 m_s m_u - l_s \omega_c^2 m_u - l_c c_t \omega_c^2 - l_s \omega_c^2 m_s - k_t \omega_c^2 m_s + l_s k_t = 0 \\ \left(-l_c m_u \omega_c^3 - l_c \omega_c^3 m_s - c_t \omega_c^3 m_s + l_s c_t \omega_c + l_c k_t \omega_c\right) j + \\ \left(\omega_c^2 m_u l_1 - \omega_c^3 m_u l_2 j - c_t l_1 j\omega_c - c_t l_2 \omega_c^2 - k_t l_1 + k_t l_2 j\omega_c\right) e^{-j\omega_c \tau_{\max}} = 0. \end{cases} \tag{51}$$

Based on the above derivations, we can separate the real part a and the imaginary part b in Equation (50) by Euler formula, and then evaluating Equation (51) yields the values of ω_c and $\tau_{\max}$ as $\omega_c = 6.71$ Hz, and $\tau_{\max} \approx 38$ ms by setting $a = 0$ and $b = 0$, respectively.

By further synthesizing the aforementioned derivations, we can get Remark 6 as follows.

Remark 6. In general, the actuator input delay usually causes the performance penalties of active suspension system in (5), and the increased input delay τ will impose the more serious impacts on vehicle suspension dynamics performance, and the obtained critical input delay $\tau_{\max}$ is useful for accessing the control performances of the designed controller. In this case, if the actuator input delay is less than the value of $\tau_{\max}$, then the proposed controller can ensure that the safety performance constraints in (6)-(8) are satisfied, which improves the ride quality and handling stability of active suspension system.

4.2 | Stability analysis of the critical delay system

Define the state variables $x_5(t) = z_s$, $x_6(t) = \dot{z}_s$, $x_7(t) = z_u$, and $x_8(t) = \dot{z}_u$, and substituting Equations (42)-(43) into Equation (45), we can get

$$\begin{cases} \dot{x}_5(t) = x_6(t) \\ \dot{x}_6(t) = \frac{1}{m_s}\left(-F_s(z_s, z_u, t) - F_c(\dot{z}_s, \dot{z}_u, t) + u(t-\tau_{\max})\right) \\ \dot{x}_7(t) = x_8(t) \\ \dot{x}_8(t) = \frac{1}{m_u}(F_s(z_s, z_u, t) + F_c(\dot{z}_s, \dot{z}_u, t) - u(t-\tau_{\max}) - k_t z_u(t) - c_t \dot{z}_u(t)), \end{cases} \tag{52}$$

where $u(t-\tau_{\max}) = l_1 z_s(t-\tau_{\max}) - l_2 \dot{z}_s(t-\tau_{\max})$.

First, the tracking error of vehicle body displacement $e_3(t)$ and its derivate are given by

$$e_3 = x_5(t), \dot{e}_3 = x_6(t). \tag{53}$$

Based on Lyapunov stability theory, define a semidefinite Lyapunov candidate function $V_4(e_3(t))$, it is easy to get $V_4(e_3(t)) \to \infty$ and when $|e_3(t)| \to \infty$, whereby $e_3(t)$ is taken as a regulated variable.

$$V_4(e_3(t)) = \frac{1}{2} e_3^2(t). \tag{54}$$

Next, let $\alpha_3(t)$ as the ideal value of $x_6(t)$, which is designed as

$$\alpha_3(t) = k_3 \tanh(e_3(t)), \tag{55}$$

where k_3 is a positive constant.

The tracking error of vehicle body velocity $e_4(t)$ is then derived as

$$e_4(t) = x_6(t) - \alpha_3(t). \tag{56}$$

By further derivation, we can obtain

$$\dot{V}_4(e_3(t)) = e_3(t) e_4(t) - k_3 e_3(t) \tanh(e_3(t)). \tag{57}$$

From (57), if $e_4(t) = 0$, we have $\dot{V}_4(e_3(t)) = -k_3 e_3(t) \tanh(e_3(t)) \le -k_3 e_3^2(t) \le 0$, and thus the asymptotical stability of $e_3(t)$ can be accordingly guaranteed.

Third, according to Equation (53) and Equation (56), define a new semidefinite Lyapunov candidate function $V_5(e_3,e_4,t)$ as

$$V_5(e_3, e_4, t) = \frac{1}{2} e_3^2 + \frac{1}{2} e_4^2. \tag{58}$$

Then, the control force with respect to $u(t-\tau_{\max})$ in Equation (52) can be rewritten as

$$\begin{aligned} u(t-\tau_{\max}) =& F_s(z_s, z_u, t) + F_c(\dot{z}_s, \dot{z}_u, t) \\ &+ m_s\left(-k_3\left(1 - \tan \mathrm{h}^2(e_3)\right)\dot{e}_3 - k_4 \tanh(e_4) - e_3\right), \end{aligned} \tag{59}$$

where k_4 is a positive constant.

Differentiating Equation (58) yields to

$$\begin{aligned} V_5(e_3, e_4, t) &= e_3(t)\dot{e}_3(t) + e_4(t)\dot{e}_4(t) \\ &= e_3(t) e_4(t) - k_3 e_3(t) \tanh(e_3(t)) + e_4(t)(\dot{x}_6(t) - \dot{\alpha}(t)) \\ &= -k_3 e_3(t) \tanh(e_3(t)) - k_4 e_4(t) \tanh(e_4(t)). \end{aligned} \tag{60}$$

TABLE 1 The parameters of quarter-vehicle active suspension system

Parameter	Value
m_s	300 kg
m_u	60 kg
k_s	15 000 N/m
k_{ns}	150 000 N/m^3
c_{s1}	1500 Ns/m
c_{s2}	1000 Ns/m
c_t	2000 Ns/m
k_t	200 000 N/m

TABLE 2 The design parameters of the adaptive backstepping controller

Parameter	$\mathbf{r}_\theta$	k_1	k_2	$\theta_{\min}$	$\theta_{\max}$
Value	0.001	10	10	1/330	1/270

It is observed from (60) that, for arbitrary parameter $k_3 > 0$ and $k_4 > 0$, we obtain $\dot{V}_5$ are uniformly continuous. Moreover, it can be derived from Lemma 1 that it is true for $\lim_{t\to\infty} \dot{V}_5 \to 0$ with $t \to \infty$, the further expressions are $\lim_{t\to\infty} e_3(t) \to 0$ and $\lim_{t\to\infty} e_4(t) \to 0$. In other words, we can arrive at the conclusion that the tracking errors of $e_3(t)$ and $e_4(t)$ will definitely tend to be asymptotic stability.

5 | SIMULATION RESULTS AND DISCUSSION

In this section, a numerical example is provided to illustrate the effectiveness of the proposed adaptive backstepping controller under bump and random road excitation. The parameters used for this simulation[32] are given in Table 1, and the initial values of the control system are set as $x_i = 0$ $(i = 1, 2, 3, 4)$, $\theta(0) = 1/270$, and the parameters of the designed controller are determined in Table 2.

To better verify the superior performance of the proposed adaptive backstepping controller in this paper, a comparative simulation is performed for the following three types of vehicle suspension systems as:

- The passive suspension, denoted as PS;
- The traditional adaptive backstepping controller, denoted as TABC;
- The proposed novel adaptive backstepping controller, denoted as NABC.

5.1 | Performance analysis of the controller under bump road

Generally, the bump road disturbance is used to mimic an isolated shock on a smooth road surface,[32] which is mathematically expressed by

$$z_{rf} = \begin{cases} \frac{h_b}{2}\left(1 - \cos\left(8\pi t\right)\right), & 1 \le t \le 1.25 \\ 0, & \text{otherwise}, \end{cases} \tag{61}$$

where $h_b = 0.03$ m is the height of road bump.

Figure 3 shows the response comparisons of the vertical acceleration and the safety constraint indicators for active suspension system with NABC under different input delays. It is observed from Figure 3A that, with the increase of input delay, there is also an increase in the vertical acceleration of vehicle body, which illustrates that the ride quality is getting worse. When the input delay gets closer to or even exceeds its maximal value $\tau_{\max} = 38$ ms, we find that the motion of vehicle body will reach into an unstable state even if the bump road disturbance disappears, which illustrates that the control failure is encountered for the closed-loop system, and meanwhile the input delay has significant negative effects on the control system. Moreover, one can obtain from Figure 3B-D that all the required safety performance conditions can be fully guaranteed. Specifically, the value of suspension defect is less than 0.15 m, the tire load ratio is less than one, and the maximal control input force does not exceed its allowed upper boundary 1000 N, which demonstrates that the proposed controller can ensure the ride stability and safety performance requirements of active suspension system in the presence of the input delay and the bump road disturbance.

Figure 4 reveals the response comparisons of the sprung-mass acceleration $\ddot{z}_c$ for the PS, TABC, and NABC systems when selecting $\tau = 0$ ms and $\tau = 20$ ms. It is observed that both of the TABC and NABC can effectively reduce the vertical acceleration of vehicle body and isolate the vibrations caused by the road disturbance compared to the PS system response in case of $\tau = 0$ ms, besides, the time evaluation of $\ddot{z}_c$ for the proposed NABC shows a smooth tendency with the smaller

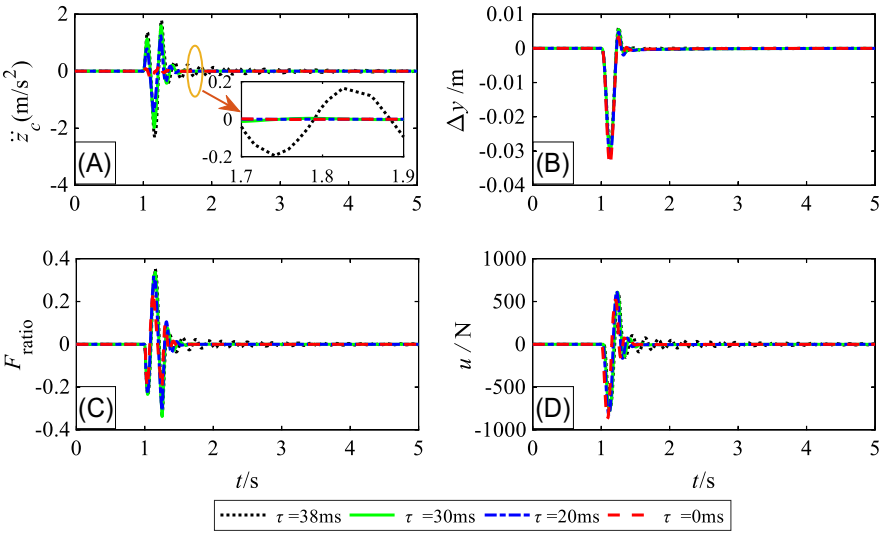

FIGURE 3 The response comparisons of the performance indicators as (a) the vertical acceleration, (b) suspension dynamic displacements, (c) tire load ratios, and (d) control forces for active suspension system with novel adaptive backstepping controller (NABC) under different input delays [Colour figure can be viewed at wileyonlinelibrary.com]

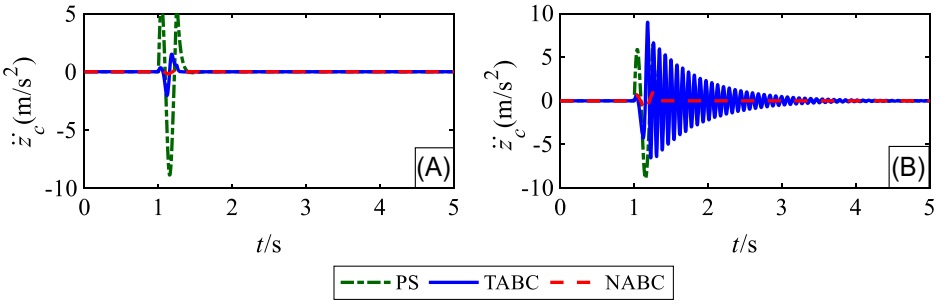

FIGURE 4 The response comparisons of the sprung-mass acceleration for the PS, TABC, and NABC suspensions when (a) $\tau = 0$ ms and (b) $\tau = 20$ ms under bump road disturbance. NABC, novel adaptive backstepping controller; PS, passive suspension; TABC, traditional adaptive backstepping controller [Colour figure can be viewed at wileyonlinelibrary.com]

TABLE 3 Root-means-square (RMS) comparisons of $\ddot{z}_c$ under bump road disturbance

Controller	$\ddot{z}_c$(m/s^2)	Changes/ % (− enhance, + worsen)
PS	1.5789	—
TABC ($\tau = 0$ ms)	0.2918	−81.52
NABC ($\tau = 0$ ms)	0.0346	−97.81
TABC ($\tau = 20$ ms)	1.7474	+9.64
NABC ($\tau = 20$ ms)	0.2027	−87.16

Abbreviations: NABC, novel adaptive backstepping controller; PS, passive suspension; TABC, traditional adaptive backstepping controller.

peak value of $\ddot{z}_c$, whereas in case of $\tau = 20$ ms, the developed NABC can well improve the ride quality of active suspension system, yet the sprung-mass acceleration $\ddot{z}_c$ for the TABC has deteriorated to a situation that is worse than that of the PS suspension, which shows that the critical input delay of TABC is less than or equal to 20 ms, and NABC can tolerate with a greater input delay.

To further demonstrate the advantages of the designed controller, when the input delay is set as $\tau = 0$ ms and $\tau = 20$ ms, Figure 5 is provided to show the power spectral density (PSD) comparisons of $\ddot{z}_c$ for active suspension system, Table 3 lists the RMS values of $\ddot{z}_c$ and Figure 6 gives the histogram comparisons of $\ddot{z}_c$ for the PS, TABC, and NABC systems. It should be noted that the calculation expression of RMS for $\ddot{z}_c$ is defined by[32]

$$\ddot{z}_c(t)_{\mathrm{RMS}} = \frac{\|\ddot{z}_c(t)\|}{\sqrt{n}} = \sqrt{\frac{1}{n}\sum_{i=1}^{n}(\ddot{z}_c(t))^2}, i = 1, \ldots, n. \tag{62}$$

According to ISO2361 criteria, the most sensitive vibration frequency of human viscera and vertebral system usually ranges from 4.0 Hz to 8.0 Hz. Therefore, it would be much better if the sprung-mass acceleration gets smaller in this

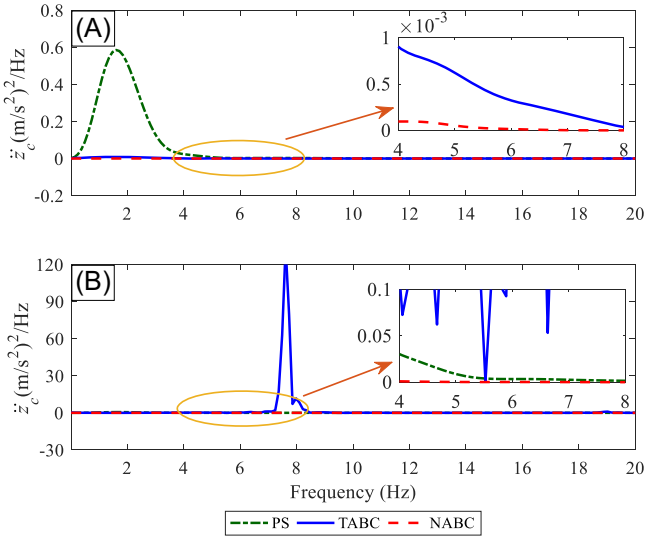

FIGURE 5 The PSD comparisons of $\ddot{z}_c$ for the PS, TABC, and NABC systems when (a) $\tau = 0$ ms and (b) $\tau = 20$ ms under bump road disturbance. NABC, novel adaptive backstepping controller; PS, passive suspension; TABC, traditional adaptive backstepping controller [Colour figure can be viewed at wileyonlinelibrary.com]

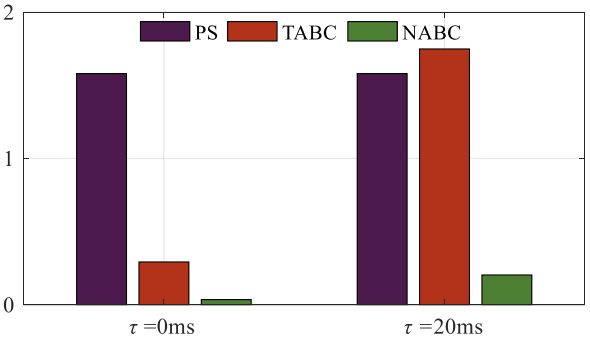

FIGURE 6 The root-means-square (RMS) histogram comparisons of $\ddot{z}_c$ for different input delays under bump road disturbance. NABC, novel adaptive backstepping controller; PS, passive suspension; TABC, traditional adaptive backstepping controller [Colour figure can be viewed at wileyonlinelibrary.com]

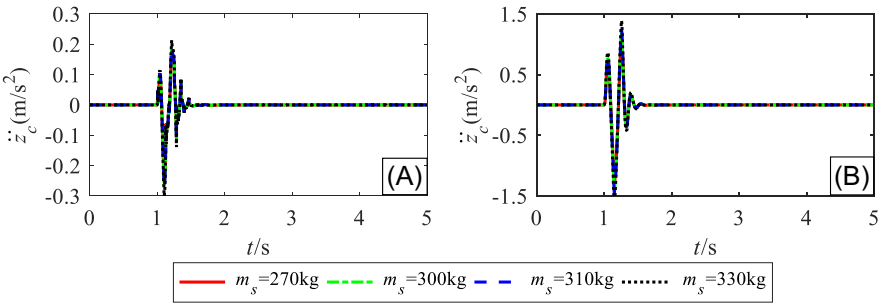

FIGURE 7 The response comparisons of $\ddot{z}_c$ for the novel adaptive backstepping controller (NABC) with different values of m_s when (a) $\tau = 0$ ms and (b) $\tau = 20$ ms under bump road disturbance [Colour figure can be viewed at wileyonlinelibrary.com]

frequency range. By analyzing the plots in Figure 5, we can easily get that the PSD response of $\ddot{z}_c$ for the NABC is better than those of the PS and TABC systems. Particularly, the PSD response of the TABC is much larger than that of the PS system in the frequency band of 7-8 Hz, which indicates that the output performances of vehicle suspension with the TABC are even getting worse than the PS system. Additionally, it can be concluded from Table 3 and Figure 6 that, compared to the corresponding acceleration in the PS system, the sprung-mass acceleration $\ddot{z}_c$ can be reduced about 81.52% and 97.81% for the TABC and NABC in case of $\tau = 0$ ms, whereas in case of $\tau = 20$ ms, $\ddot{z}_c$ is increased about 9.64% for the TABC and is reduced about 87.16% for the NABC system.

It can be concluded from Figures 4 to 6 and Table 3 that, compared to the TABC, our designed NABC can generate obvious improvements for vehicle body acceleration regardless if $\tau = 0$ ms or $\tau = 20$ ms under bump road disturbance, and the NABC can tolerant with greater input delay under a certain external road disturbance and retain better dynamics performance for active suspension system.

To further analyze the variation of $\ddot{z}_c$ for the proposed NABC with changing m_s, the simulation is conducted and the results are shown in Figure 7. It can be observed that the changes in m_s have a little impact on the sprung-mass acceleration for the NABC.

5.2 | Performance analysis of the controller under random road

The random road disturbance can also be employed to carry out the comparative simulation, and it is often assumed as a vibration signal that is consistent and typically specified by[42]

$$\dot{q}(t) = -2\pi f_0 q(t) + 2\pi n_0 \omega(t) \sqrt{G_q(n_0)\, v}, \tag{63}$$

where f_0 is the lower cut-off frequency of road profile, n_0 is the reference spatial frequency with a constant value of $n_0 = 0.1(1/\mathrm{m})$, $G_q(n_0)$ is the road roughness coefficient, $\omega(t)$ is a Gauss white noise of unit intensity. In this case, we choose $G_q(n_0) = 64 \times 10^{-6}\ \mathrm{m}^3$ as B-class road, and $v = 72$ (km/h).

Herein, the simulation is conducted for the designed NABC under random road disturbance and different input delays, and the simulation results are presented in Figure 8.

One can obtain that the sprung-mass acceleration of $\ddot{z}_c$ shows an increasing variation when the input delay gets larger from 0 to 38 ms, whereas the safety performance constrains are all basically remained in a relative stability state for the various input delays and are satisfied with the performance requirements of active suspension system, which illustrates the NABC can well reduce the vibration effects caused by the actuator input delay.

On the other hand, the simulation results of $\ddot{z}_c$ and its corresponding PSD variation are provided in Figure 9 and Figure 10 to show the response comparisons of the PS, TABC, and NABC systems by choosing $\tau = 0$ ms and $\tau = 20$ ms under random road disturbance.

As it is shown in Figure 9, compared to the PS system, both of TABC and NABC can obviously reduce the amplitude of $\ddot{z}_c$, whereas the latter one has a gentler and smaller acceleration curve. Additionally, it is seen from Figure 10 that, regardless if the input delay is set as $\tau = 0$ ms and/or $\tau = 20$ ms, both of the PSD responses of $\ddot{z}_c$ for the TABC and NABC are all less than those of the PS system in the concerned frequency band. Moreover, the superiority of the designed NABC is more obvious than that of the TABC.

In a similar way, Table 4 summarizes the RMS values of $\ddot{z}_c$ and Figure 11 displays the histogram comparisons of $\ddot{z}_c$ for the PS, TABC, and NABC systems. As shown in Table 4, the RMS values of $\ddot{z}_c$ with the TABC and NABC can be reduced about 93.34%, 98.49% and 79.87%, 87.47%, respectively, compared to the PS system in case of $\tau = 0$ ms and/or $\tau = 20$ ms,

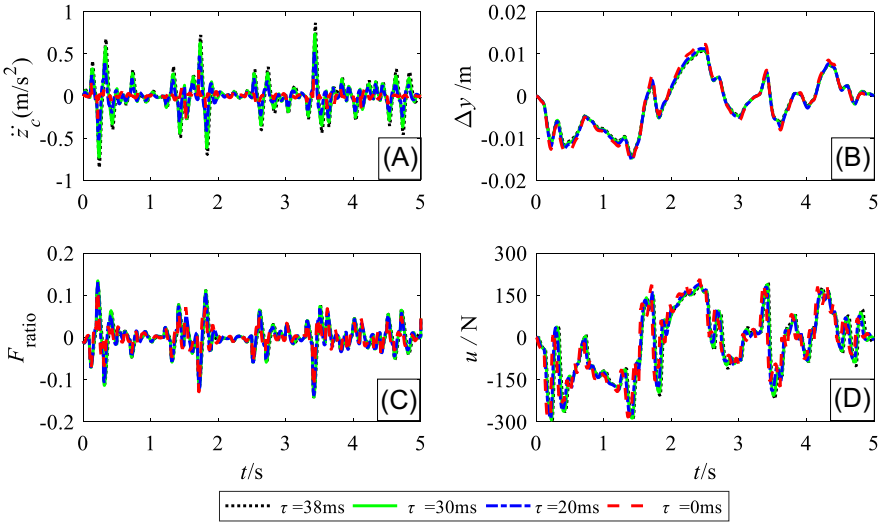

FIGURE 8 The response comparisons of the dynamics indicators as (a) the vertical accelerations, (b) suspension dynamic displacements, (c) tire load ratios, and (d) control forces for active suspension system with novel adaptive backstepping controller (NABC) under different input delays [Colour figure can be viewed at wileyonlinelibrary.com]

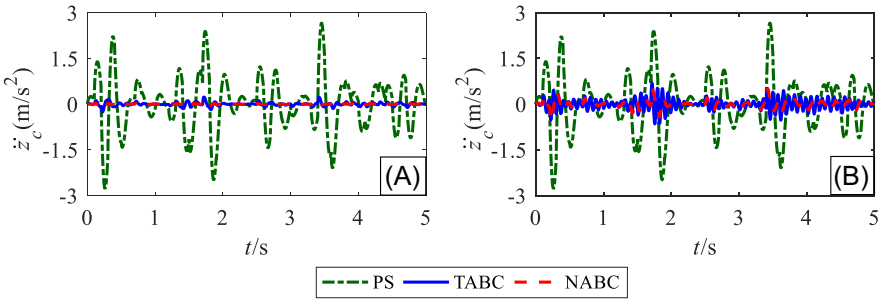

FIGURE 9 The response comparisons of $\ddot{z}_c$ for the PS, TABC, and NABC systems when (a) $\tau = 0$ ms and (b) $\tau = 20$ ms under random road disturbance. NABC, novel adaptive backstepping controller; PS, passive suspension; TABC, traditional adaptive backstepping controller [Colour figure can be viewed at wileyonlinelibrary.com]

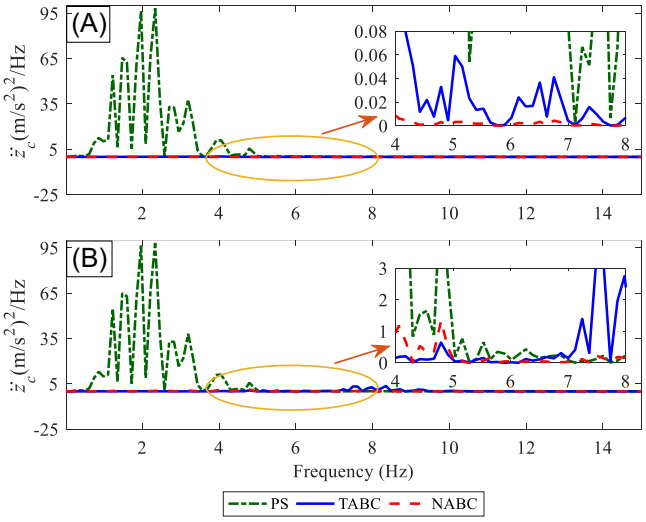

FIGURE 10 The PSD comparisons of $\ddot{z}_c$ for the PS, TABC, and NABC systems when (a) $\tau = 0$ ms and (b) $\tau = 20$ ms under random road disturbance. NABC, novel adaptive backstepping controller; PS, passive suspension; TABC, traditional adaptive backstepping controller [Colour figure can be viewed at wileyonlinelibrary.com]

Controller	$\ddot{z}_c$(m/s^2)	Changes/ % (− enhance, + worsen)
PS	0.8877	—
TABC ($\tau = 0$ ms)	0.0591	−93.34
NABC ($\tau = 0$ ms)	0.0134	−98.49
TABC ($\tau = 20$ ms)	0.1787	−79.87
NABC ($\tau = 20$ ms)	0.1112	−87.47

Abbreviations: NABC, novel adaptive backstepping controller; PS, passive suspension; TABC, traditional adaptive backstepping controller.

TABLE 4 Root-means-square (RMS) comparisons of $\ddot{z}_c$ under random road disturbance

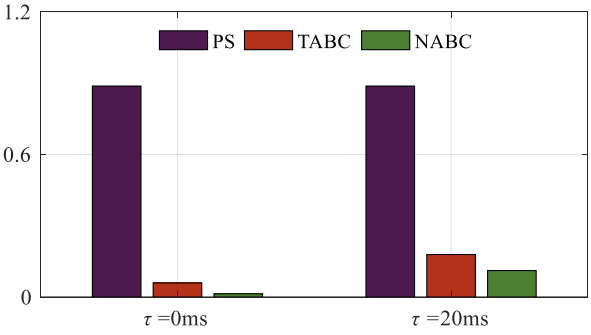

FIGURE 11 The root-means-square (RMS) histogram comparisons of $\ddot{z}_c$ for different input delays under random road disturbance. NABC, novel adaptive backstepping controller; PS, passive suspension; TABC, traditional adaptive backstepping controller [Colour figure can be viewed at wileyonlinelibrary.com]

which indicates that the control performance of the designed NABC is overall better than that of the TABC with satisfying the safety performance constraints under random road profiles.

From the simulation results in Figures 9 to 11 and Table 4, compared with the TABC, it is clear that the vehicle body acceleration with the NABC can be significantly enhanced whether there exists the actuator input delay or not, compared with the TABC, which indicates that our proposed NABC can effectively prevent the resonance caused by the road surface and the human body, and provide much better ride quality.

Figure 12 shows the variation of $\ddot{z}_c$ with different values of m_s, and it can be observed that the changes in m_s have almost no effect on the suspension performances for the NABC in the presence of random road disturbance, which further illustrates that the proposed NABC has a good adaptive control effect for this active suspension system. In summary, regardless of how to choose the values of input delay (0-38 ms), the proposed controllers can guarantee the suspension safety performance constraints under random road disturbance.

5.3 | Actuator power consumption

In order to evaluate the power consumption for the different control schemes, the actuator power demand is mathematically expressed by the RMS of the positive mechanical power generating from the active control force $u(t - \tau)$ and its

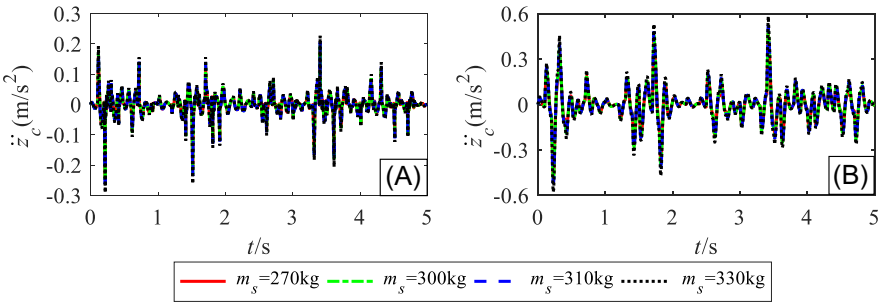

FIGURE 12 The response comparisons of $\ddot{z}_c$ for the novel adaptive backstepping controller (NABC) with different values of m_s when (a) $\tau = 0$ ms and (b) $\tau = 20$ ms under random road disturbance [Colour figure can be viewed at wileyonlinelibrary.com]

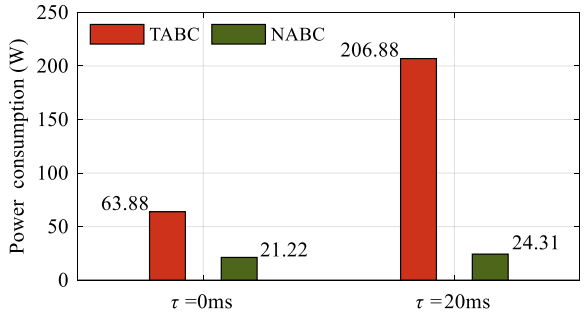

FIGURE 13 The response of power consumption for the TABC and NABC when (a) $\tau = 0$ ms and (b) $\tau = 20$ ms under bump road disturbance. NABC, novel adaptive backstepping controller; TABC, traditional adaptive backstepping controller [Colour figure can be viewed at wileyonlinelibrary.com]

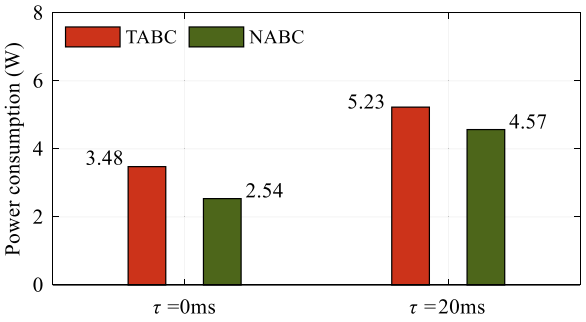

FIGURE 14 The response of power consumption for the TABC and NABC when (a) $\tau = 0$ ms and (b) $\tau = 20$ ms under random road disturbance. NABC, novel adaptive backstepping controller; TABC, traditional adaptive backstepping controller [Colour figure can be viewed at wileyonlinelibrary.com]

velocity $\dot{z}_s - \dot{z}_u$ with respect to the input delay as[18]

$$P^{+}_{\mathrm{RMS}}(t) = \frac{\|P^{+}(t)\|}{\sqrt{n}} = \sqrt{\frac{1}{n}\sum_{i=1}^{n}\left(P^{+}(t)\right)^2}\ i = 1, \ldots, n, \tag{64}$$

where

$$P^{+}(t) = \begin{cases} u(t-\tau)\left(\dot{z}_s - \dot{z}_u\right), u(t-\tau)\left(\dot{z}_s - \dot{z}_u\right) > 0 \\ 0, \qquad\qquad \text{otherelse.} \end{cases}$$

Figures 13 and 14 reveals the power consumption of active suspension system with the TABC and NABC when the input delay is set as $\tau = 0$ ms and $\tau = 20$ ms.

It can be observed that, regardless of the presence of bump or random road disturbance, the proposed NABC could have much less power consumption compared with the TABC under the same ride quality situation. At the same time, the power consumptions for the TABC and NABC under random road are overall less than those under bump road, which reflects that the proposed NABC should at least meet the performance requirements for this active suspension system under bump road.

It can be concluded from Section 5 that, regardless if the input delay is considered or not, the proposed NABC can effectively improve the dynamics performance of the controlled active suspension system and has better adaptive control effect and lower energy consumption, as long as the input delay disturbance is less than the critical time delay $\tau_{\max}$. In addition to this, the proposed NABC can tolerant with greater input delay in comparison with the TABC. More specifically, the proposed controller can effectively suppress the negative impacts of the system nonlinearities, the parameter uncertainties, as well as the input delays on active suspension system.

6 | CONCLUSIONS

In this paper, a novel adaptive backstepping-based control design is proposed for uncertain nonlinear active suspension system with the input delay. A nonlinear dynamics model of quarter-vehicle suspension is first established by considering the actuator input delay and the safety performance constraints for active suspension system in the presence of the sprung-mass uncertainties. Then, based on this model, an adaptive control law is designed to meet the requirements of suspension safety constraints. Meanwhile, the stability analysis of zero dynamics is conducted to guarantee the boundedness of the safety constraint performances. Moreover, a simple and effective method for calculating the critical input delay is presented through deriving the relationship between the actuator input delay and the state variables of active suspension system. Finally, a simulation investigation is performed to show the effectiveness of the designed adaptive backstepping controller. Future study will focus on the development of implementation of the hardware-in-loop controller. Our future work will focus on the multiobjective coordinated optimization control over the performance indicators including sprung-mass acceleration, suspension dynamic displacement, and tire dynamic load on the active suspension system.

ACKNOWLEDGEMENTS

This work is supported by the National Natural Science Foundation of China (grants 51675423 and 51305342) and by the Primary Research & Development Plan of Shannxi Province (grant 2017GY-029).

CONFLICT OF INTEREST

The authors of this paper declare that they have no conflict of interest.

NOTES

This paper is compliant with ethical standards.

ORCID

Hui Pang https://orcid.org/0000-0001-7550-8376

REFERENCES

1. Cao D, Song X, Ahmadian M. Editors' perspectives: road vehicle suspension design, dynamics, and control. *Veh Syst Dyn*. 2011;49(1-2):3-28.
2. Kong Y, Zhao D, Yang B, Han C, Han K. Robust non-fragile $H_\infty / L_2 - L_\infty$ control of uncertain linear system with time-delay and application to vehicle active suspension. *Int J Robust Nonlinear Control*. 2015;25(13):2122-2141.
3. Guan Y, Han Q, Yao H, Ge X. Robust event-triggered H_∞ controller design for vehicle active suspension systems. *Nonlinear Dynamics*. 2018;94(1):627-638.
4. Sun W, Gao H, Kaynak O. Finite frequency H_∞ control for vehicle active suspension systems. *IEEE Trans Control Syst Technol*. 2011;19(2):416-422.
5. Gysen B, Paulides J, Janssen J, Lomonova E. Active electromagnetic suspension system for improved vehicle dynamics. *IEEE Trans Veh Technol*. 2010;59(3):1156-1163.
6. Huang S, Lin W. Adaptive fuzzy controller with sliding surface for vehicle suspension control. *IEEE Trans Fuzzy Syst*. 2003;11(4):550-559.
7. Khan L, Qamar S, Khan M. Adaptive wavelets based fuzzy NN control for active suspension model. In: *Emerging Trends and Applications in Information Communication Technologies: Second International Multi Topic Conference, IMTIC 2012, Jamshoro, Pakistan, March 28-30, 2012. Proceedings*. Berlin, Germany: Springer-Verlag Berlin Heidelberg; 2012:249-260. *Communications in Computer and Information Science*; vol. 281.
8. Guo L, Zhang L. Robust H_∞ control of active vehicle suspension under non-stationary running. *J Sound Vib*. 2012;331(26):5824-5837.
9. Ferrara A, Incremona GP, Regolin E. Optimization-based adaptive sliding mode control with application to vehicle dynamics control. *Int J Robust Nonlinear Control*. 2019;29(3):550-564.
10. Kilicaslan S. Control of active suspension system considering nonlinear actuator dynamics. *Nonlinear Dynamics*. 2018;91(2):1383-1394.
11. Lin J, Huang C. Nonlinear backstepping control design of half-car active suspension systems. *Int J Veh Des*. 2003;33(4):332-350.
12. El Majdoub K, Giri F, Chaoui F. Backstepping adaptive control of quarter-vehicle semi-active suspension with Dahl MR damper model. *IFAC Proc Vol*. 2013;46(11):558-563.
13. Lian R. Enhanced adaptive self-organizing fuzzy sliding-mode controller for active suspension systems. *IEEE Trans Ind Electron*. 2013;60(3):958-968.

14. Li H, Jing X, Karimi HR. Output-feedback-based H_∞ control for vehicle suspension systems with control delay. *IEEE Trans Ind Electron*. 2014;61(1):436-446.
15. Bucak İÖ, Öz HR. Vibration control of a nonlinear quarter-car active suspension system by reinforcement learning. *Int J Syst Sci*. 2012;43(6):1177-1190.
16. Deshpande VS, Shendge PD, Phadke SB. Dual objective active suspension system based on a novel nonlinear disturbance compensator. *Veh Syst Dyn*. 2016;54(9):1269-1290.
17. Sun W, Pan H, Zhang Y, Gao H. Multi-objective control for uncertain nonlinear active suspension systems. *Mechatronics*. 2014;24(4):318-327.
18. Pan H, Jing X, Sun W. Robust finite-time tracking control for nonlinear suspension systems via disturbance compensation. *Mech Syst Signal Process*. 2017;88:49-61.
19. Sakthivel R, Arunkumar A, Mathiyalagan K, Selvi S. Robust reliable control for uncertain vehicle suspension systems with input delays. *J Dyn Syst Meas Control*. 2015;137(4):041013.
20. Deng W, Yao J, Ma D. Time-varying input delay compensation for nonlinear systems with additive disturbance: an output feedback approach. *Int J Robust Nonlinear Control*. 2018;28(1):31-52.
21. Leite V, Peres P. Pole location control design of an active suspension system with uncertain parameters. *Veh Syst Dyn*. 2005;43(8):561-579.
22. Khan L, Qamar S, Khan M. Comparative analysis of adaptive NeuroFuzzy control techniques for full car active suspension system. *Arab J Sci Eng*. 2014;39(3):2045-2069.
23. Nguyen TT, Bui TH, Tran TP, Kim SB. A hybrid control of active suspension system using H_∞ and nonlinear adaptive controls. Paper presented at: 2001 IEEE International Symposium on Industrial Electronics Proceedings (ISIE); 2001; Pusan, South Korea.
24. Ahn K, Nam D, Jin M. Adaptive backstepping control of an electrohydraulic actuator. *IEEE/ASME Trans Mechatron*. 2013;19(3):987-995.
25. Zapateiro M, Luo N, Karimi H, Vehi J. Vibration control of a class of semiactive suspension system using neural network and backstepping techniques. *Mech Syst Signal Process*. 2009;23(6):1946-1953.
26. Ali M, Saravanakumar R. Novel delay-dependent robust H_∞ control of uncertain systems with distributed time-varying delays. *Appl Math Comput*. 2014;249:510-520.
27. Du H, Zhang N. Constrained H_∞ control of active suspension for a half-car model with a time delay in control. *Proc Inst Mech Eng D J Automob Eng*. 2008;222(5):665-684.
28. Li H, Liu H, Hand S, Hilton C. Multi-objective H_∞ control for vehicle active suspension systems with random actuator delay. *Int J Syst Sci*. 2012;43(12):2214-2227.
29. Du H, Zhang N, Lam J. Parameter-dependent input-delayed control of uncertain vehicle suspensions. *J Sound Vib*. 2008;317(3-5):537-556.
30. Sun W, Zhao Y, Li J, Zhang L, Gao H. Active suspension control with frequency band constraints and actuator input delay. *IEEE Trans Ind Electron*. 2011;59(1):530-537.
31. Wang Y, Li Y, Zheng L. Backstepping and Smith predictor integrated control on MR vehicle suspension system. Paper presented at: IEEE 2011 International Conference on Electrical and Control Engineering (ICECE); 2011; Yichang, China.
32. Yagiz N, Hacioglu Y. Backstepping control of a vehicle with active suspensions. *Control Eng Pract*. 2008;16(12):1457-1467.
33. Sun W, Gao H, Kaynak O. Adaptive backstepping control for active suspension systems with hard constraints. *IEEE/ASME Trans Mechatron*. 2012;18(3):1072-1079.
34. Pan H, Sun W. Nonlinear output feedback finite-time control for vehicle active suspension systems. *IEEE Trans Ind Inform*. 2019;15(4):2073-2082.
35. Pan H, Sun W, Gao H, Yu J. Finite-time stabilization for vehicle active suspension systems with hard constraints. *IEEE Trans Intell Transp Syst*. 2015;16(5):2663-2672.
36. Sun M. A Barbalat-like lemma with its application to learning control. *IEEE Trans Autom Control*. 2009;54(9):2222-2225.
37. Yao B, Bu F, Reedy J, Chiu G. Adaptive robust motion control of single-rod hydraulic actuators: theory and experiments. *IEEE/ASME Trans Mechatron*. 2000;5(1):79-91.
38. Yao B, Tomizuka M. Adaptive robust control of MIMO nonlinear systems in semi-strict feedback forms. *Automatica*. 2001;37(9):1305-1321.
39. Elin M, Shoikhet D. *Linearization Models for Complex Dynamical Systems: Topics in Univalent Functions, Functional Equations and Semigroup Theory*. Basel, Switzerland: Birkhäuser Verlag; 2010.
40. Arimoto S. *Control Theory of Non-Linear Mechanical Systems*. Oxford, UK: Oxford University Press; 1996.
41. Habibullah H, Pota H, Petersen I, Rana M. Tracking of triangular reference signals using LQG controllers for lateral positioning of an AFM scanner stage. *IEEE/ASME Trans Mechatronics*. 2014;19(4):1105-1114.
42. Pang H, Fu W, Liu K. Stability analysis and fuzzy smith compensation control for semi-active suspension systems with time delay. *J Intell Fuzzy Syst*. 2015;29(6):2513-2525.

How to cite this article: Pang H, Zhang X, Yang J, Shang Y. Adaptive backstepping-based control design for uncertain nonlinear active suspension system with input delay. *Int J Robust Nonlinear Control*. 2019;1–20. https://doi.org/10.1002/rnc.4695